

Dynamics of 9-Hydroxyphenalenone Studied by One-Dimensional Solid-State Spin Exchange NMR

Daisuke Kuwahara,^{*,†} Hiroyuki Koyano,[†] Taisuke Manaka,[†] Hideaki Nakamura,[†] Tomoyuki Mochida,[§] and Tadashi Sugawara[‡]

The University of Electro-Communications, 1-5-1 Chofugaoka, Chofu-shi, Tokyo 182-8585, Japan, Department of Chemistry, Faculty of Science, Toho University, Funabashi, Chiba 274-8510, Japan, and Department of Basic Science, Graduate School of Arts and Sciences, The University of Tokyo, 3-8-1 Komaba, Meguro, Tokyo 153-8902, Japan

Received: August 19, 2006; In Final Form: October 25, 2006

We present a new NMR method to clarify the dynamics of proton tautomerism in solid 9-hydroxyphenalenone. Two ¹³C resonance lines influenced by the proton tautomerism have a chemical-shift difference between them, which increases with decreasing temperature. To depict the precise potential curve of the proton tautomerism, the chemical-shift difference when the proton tautomerism is completely frozen is necessary. For solid 9-hydroxyphenalenone and its derivatives, the freezing temperatures are often under -100 °C. When the freezing temperatures are below the temperature range in which standard magic angle spinning NMR probes can perform a sample spinning, it is very difficult to obtain the shift difference. The NMR experiments based on this new method are performed at a temperature significantly higher than -100 °C at which the proton tautomerism is still active. The new method yields the ¹³C spin relaxation rates, the rates for the proton tautomerism, and the populations of the two tautomers. Using the populations and the ¹³C chemical-shift difference at that temperature, we determined the chemical-shift difference at the freezing temperature. We also obtained several parameters characterizing the potential profile for the proton dynamics in solid 9-hydroxyphenalenone.

1. Introduction

9-Hydroxyphenalenone derivatives show dielectric responses based on the tautomerism in crystals. The tautomerism is induced synchronizing with the proton transfer. Recently, the phase transition behaviors have been reported by Mochida et al.;^{1–3} they showed that the dielectric responses of these derivatives were caused by the polarization reversing associated with the proton tautomerism.

An intra- or intermolecular hydrogen bond is one of the important factors that produce the proton tautomerism in the solid state. For the 9-hydroxyphenalenone derivatives, the proton transfer takes place along an intramolecular hydrogen bond.^{1–3} In addition, the molecules can be considered as isolated systems having a hydrogen bond. They are, therefore, ideal systems to study the association between the proton tautomerism due to the hydrogen bond and the dielectric responses.

Much attention has recently focused on tautomerism, because it has potential applications in molecular devices.⁴ A memory function device is a representative example of such devices. The 9-hydroxyphenalenone derivatives also have proton tautomerism in their crystals. Thus, if we can control this phenomenon, they may be available as memory function devices.

To properly control the proton tautomerism, we require detailed information on the potential profile of the proton

transfer. Figure 1 shows a schematic representation of the potential curve for the proton tautomerism. The dynamics of the proton transfer is highly dependent on the shape along the reaction coordinate. In general, the following parameters are used to specify the potential curve: the exchange rates, k_1 and k_{-1} , the energy difference, ΔG , and the activation energy, ΔG^\ddagger . Two tautomers of 9-hydroxyphenalenone are depicted in Figure 1. Whereas they are bilaterally symmetric, they have a potential energy difference due to the difference in their crystallographic environments.

Limbach et al. have studied the dynamics of the proton tautomerism of porphyrin derivatives.^{5,6} In their study, ¹⁵N magic angle sample spinning (MAS) NMR spectra were measured at several temperatures; the splitting width, $\delta\nu$, of the two resonance lines corresponding to the two kinds of ¹⁵N sites were found to decrease with temperature. They showed that the equilibrium constant, K , for the proton tautomerism and the populations of the two tautomers were determined by the splitting width, $\delta\nu$, of the two resonance lines. The splitting width, $\delta\nu$, at a given temperature can be written as^{6,7}

$$\delta\nu = \frac{1-K}{1+K}\Delta\nu \quad (1)$$

where $\Delta\nu$ is the chemical-shift difference when the proton tautomerism is completely frozen; in what follows, the term “the stationary splitting width” is used to refer to $\Delta\nu$. Using this expression, they clarified the potential profiles (at several temperatures) for tetraphenylporphyrin.⁵

However, to employ eq 1, we have to know the stationary splitting width, $\Delta\nu$. In the case of 9-hydroxyphenalenone, its

* Corresponding author. Tel: +81 424 43 5730. Fax: +81 424 43 5501. E-mail address: kuwahara@cia.uec.ac.jp.

[†] The University of Electro-Communications.

[‡] The University of Tokyo.

[§] Toho University.

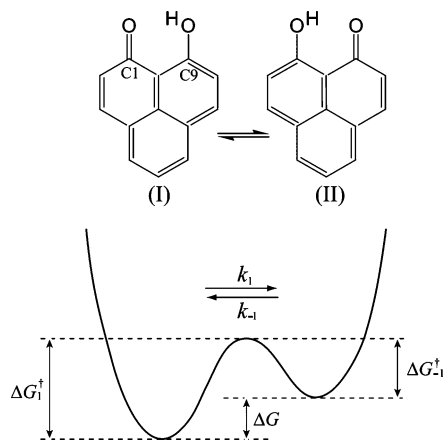


Figure 1. Potential curve for the proton transfer between two tautomers, I and II, of 9-hydroxyphenalenone. k_1 and k_{-1} are the exchange rates between the two tautomers. ΔG_1^\ddagger and ΔG_{-1}^\ddagger denote the activation energies; and ΔG is the energy difference between the two tautomers.

freezing temperature is less than -100 °C. In addition, the freezing temperatures for its derivatives are also often under -100 °C. If the freezing temperatures are below the range in which standard MAS NMR probes can perform a sample spinning, it is very difficult to obtain the shift difference, $\Delta\nu$. In such cases, we cannot obtain the precise value of $\Delta\nu$ unless a special MAS probehead, such as a Doty Super-VT MAS probe,⁸ is available; it is rare for us to find such a MAS probehead in most NMR laboratories.

In this study, we present a new method to evaluate the stationary splitting width, $\Delta\nu$, on the basis of MAS NMR experiments. We use a combination of the following two methods: cross-polarization magic angle spinning (CP/MAS) and one-dimensional (1D) solid-state spin exchange NMR. A new pulse sequence to acquire the exchange rates (k_1 and k_{-1}), relaxation rates, and populations of the two tautomers will be shown along with the detailed dynamics of the ^{13}C magnetization vectors. All the NMR experiments are performed at a manageable temperature above the lower limit. Several parameters at the temperature associated with the potential profile for 9-hydroxyphenalenone will be obtained using this new NMR method.

2. Method

The equilibrium constant, K , for the proton tautomerism is given by^{6,7}

$$K = k_1/k_{-1} = x_2/x_1 \quad (2)$$

where x_1 and x_2 are the populations for tautomers I and II, respectively. Hence, the measurement of the two rate constants, k_1 and k_{-1} , or the determination of a population x_i ($i = 1$ or 2) gives the equilibrium constant K . The NMR method presented in this study consists of the following steps: (i) both k_1 and k_{-1} or x_i are determined at a manageable temperature above -100 °C using a new 1D spin exchange NMR. (ii) A CP/MAS experiment is performed at the same temperature to obtain the splitting width $\delta\nu$. (iii) After the rate constants, k_1 and k_{-1} , or a population x_i is known, the stationary splitting width, $\Delta\nu$, is calculated from eq 1 using the splitting width, $\delta\nu$.

It is well-known that 2D exchange NMR experiments yield the rate constants for chemical exchange.^{9,10} The 2D NMR experiments are, however, too time-consuming in general, so that the experiments at a low temperature under 0 °C require a

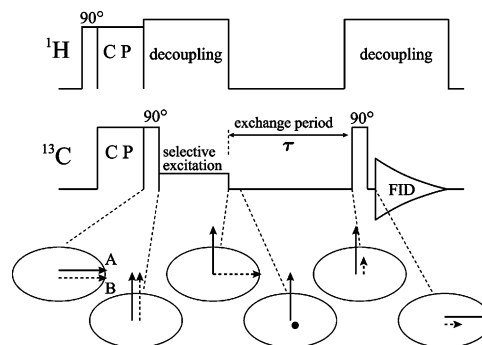


Figure 2. 1D spin exchange NMR pulse sequence devised in this study and diagram of ^{13}C magnetization vectors driven by this pulse sequence. CP denotes cross polarization. A selective excitation is realized using a soft pulse in this study. See text concerning the details of the magnetization dynamics.

great deal of nitrogen gas. Furthermore, it is necessary to plot the data points corresponding to several exchange periods to determine the rate constants. This means that several 2D NMR experiments have to be performed. For these reasons, it is favorable that the spin exchange NMR experiments can be made in a 1D scheme.

Figure 2 shows a pulse sequence devised in this study. The two vectors under the pulse sequence represent the magnetizations for carbons C1 and C9. In what follows, the magnetizations for carbons C1 and C9 are referred to as magnetizations A and B, respectively; and the resonance lines for carbons C1 and C9 are called resonances A and B, respectively. Through CP, the two magnetizations are generated in the x -direction in the rotating frame. A hard 90° pulse is applied to the carbon nuclei just after CP. As a result, the two magnetizations flip back to the $+z$ or $-z$ direction depending on the phase of the hard pulse. A frequency-selective soft pulse¹¹ is then irradiated on resonance B, and only magnetization B is moved on the transverse plane (to the x -direction). Because a strong local field exists in the exchange period, magnetization B disappears within a few milliseconds. On the other hand, a part of magnetization A is transferred to magnetization B in the exchange period owing to the proton tautomerism. At the end of the exchange period, a nonselective 90° pulse is applied to the carbon nuclei. Finally, not only resonance A but also resonance B are detected.

When magnetization A is locked in the $+z$ direction, the z -component of magnetization A just after the exchange period is written as^{6,9,12}

$$M_{A,z}^{(A,+z)}(\tau) = \frac{1}{2}M_A^{\text{eq}}(1 + (\alpha - 1)e^{-k_A\tau}) + \frac{1}{2}\alpha M_{A(I)}^{\text{eq}} \cdot e^{-k_1\tau} + \frac{1}{2}\alpha M_{A(II)}^{\text{eq}} \cdot e^{-k_{-1}\tau} \quad (3)$$

Here, τ is the exchange period and $k_A = 1/T_{1A}$, where T_{1A} is the longitudinal relaxation time of magnetization A. $M_{A(I)}^{\text{eq}}$ and $M_{A(II)}^{\text{eq}}$ are the equilibrium magnetizations corresponding to resonance A; they come from tautomers I and II, respectively. M_A^{eq} is the total equilibrium magnetization for resonance A: $M_A^{\text{eq}} = M_{A(I)}^{\text{eq}} + M_{A(II)}^{\text{eq}}$. An enhancement factor α , which is due to CP, is given by

$$M_{A,z}^{(A,+z)}(0) = \alpha M_A^{\text{eq}} \quad (4)$$

Note that α and M_A^{eq} can be experimentally determined. The line intensity of resonance A is proportional to $M_{A,z}^{(A,+z)}(\tau)$.

On the other hand, when locked in the $-z$ direction, the z -component of magnetization A is given by

$$M_{A,z}^{(A,-z)}(\tau) = \frac{1}{2}M_A^{\text{eq}}(1 - (\alpha + 1)e^{-k_A\tau}) - \frac{1}{2}\alpha M_{A(I)}^{\text{eq}} \cdot e^{-k_1\tau} - \frac{1}{2}\alpha M_{A(II)}^{\text{eq}} \cdot e^{-k_{-1}\tau} \quad (5)$$

The summation of eqs 3 and 5 leads to

$$M_{A,z}^{(A,+z)}(\tau) + M_{A,z}^{(A,-z)}(\tau) = M_A^{\text{eq}}(1 - e^{-k_A\tau}) \quad (6)$$

Equation 6 can be rewritten as

$$M_A^{\text{eq}} \cdot e^{-k_A\tau} = M_A^{\text{eq}} - M_{A,z}^{(A,+z)}(\tau) - M_{A,z}^{(A,-z)}(\tau) \quad (7)$$

Therefore, if we plot the natural logarithm of the right-hand side versus the exchange period, we can determine the longitudinal relaxation rate, $k_A = 1/T_{1A}$.

Next, we focus on resonance B. When magnetization A is locked in the $+z$ direction, the z -component of magnetization B just after the exchange period is written as

$$M_{B,z}^{(A,+z)}(\tau) = \frac{1}{2}M_A^{\text{eq}}(1 + (\alpha - 1)e^{-k_A\tau}) - \frac{1}{2}\alpha M_{A(I)}^{\text{eq}} \cdot e^{-k_1\tau} - \frac{1}{2}\alpha M_{A(II)}^{\text{eq}} \cdot e^{-k_{-1}\tau} \quad (8)$$

Subtracting eq 8 from eq 3, we obtain the following expression:

$$M_{A,z}^{(A,+z)}(\tau) - M_{B,z}^{(A,+z)}(\tau) = M_{+1} \cdot e^{-k_1\tau} + M_{-1} \cdot e^{-k_{-1}\tau} \quad (9)$$

where $M_{+1} = \alpha M_{A(I)}^{\text{eq}}$ and $M_{-1} = \alpha M_{A(II)}^{\text{eq}}$. Finally, a least-squares fit of the experimental data (for the left-hand side of eq 9) to eq 9 gives the exchange rates, k_1 and k_{-1} . Once k_1 and k_{-1} are known, the stationary splitting width can be calculated from eq 1.

To determine the relaxation rate, $k_B = 1/T_{1B}$, the 1D spin exchange NMR experiment has to be performed as follows: a frequency-selective soft pulse is applied to resonance B, and after that the line intensities of resonances B and A have to be recorded. The subscript "A" is changed to "B" in eqs 3–7 to derive the expressions for $M_{B,z}^{(B,+z)}(\tau)$, $M_{B,z}^{(B,-z)}(\tau)$, and $M_B^{\text{eq}} \cdot e^{-k_B\tau}$. If we are in line with the procedure described in the preceding paragraph with these expressions, we can then obtain the relaxation rate, k_B .

In general, a soft pulse on one resonance may affect the other resonance. This problem leads to a slight change in the enhancement factor, α , in eqs 3–5, 8, and 9 in this section. Then it can be considered that α has changed to α' in eqs 3–5, 8, and 9. Hence, this problem does not affect the rate constants obtained (i.e., the exchange rates and the relaxation rates). Furthermore, from eq 7, it can be easily understood that the different CP efficiencies for resonances A and B do not affect the relaxation rates obtained. When the exchange periods are small compared to the relaxation times, we also see from eqs 3 and 8 that the different CP efficiencies do not exert an effect upon the precision of the exchange rates obtained.

The new method presented in this section was developed from a simple picture for the ^{13}C magnetization vectors affected by the proton tautomerism. Figure 3 shows the picture for the ^{13}C magnetization dynamics. In this figure, it is assumed that a selective-excitation pulse (a soft pulse) is applied to magnetization B. Just after the exchange period, magnetization B is brought back in the $+z$ direction because of the spin relaxation. In addition, a part of magnetization A locked in the $+z$ or $-z$ direction merges with magnetization B owing to the spin exchange. Consequently, magnetization B just after the exchange

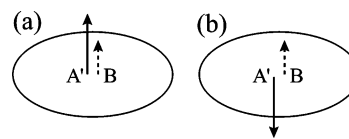


Figure 3. Simple picture that represents the ^{13}C magnetizations just after the exchange period. It is assumed that magnetization A was locked in the z ($+z$ or $-z$) direction. Only the magnetizations for carbon B are considered in this picture. Magnetization B is generated by the spin relaxation of carbon B, and magnetization A' is brought about by the proton tautomerism (the proton transfer). The resultant magnetization for carbon B can be considered to be the sum of the two magnetizations in this rough approximation.

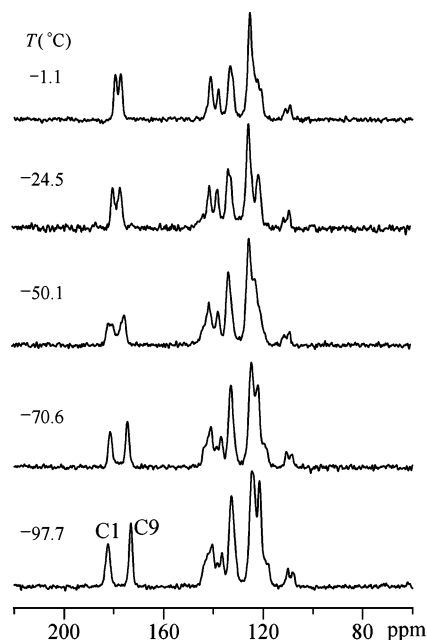


Figure 4. CP/MAS NMR spectra of 9-hydroxyphenalenone at the different indicated temperatures. The two resonance lines in the vicinity of 180 ppm correspond to C1 and C9 carbons. The resonance lines for C1 and C9 are called resonance A and resonance B in this study, respectively.

period becomes the sum of the two magnetizations. Thus, if this picture is valid, the experimental results without the effects of the spin exchange can be obtained when the two results for Figure 3a,b are added. In fact, the present figure is a fairly good approximation for the ^{13}C magnetization dynamics. This simple picture suggests that two different experiments for each magnetization are necessary to separately determine the relaxation rate and exchange rates.

3. Experimental Section

The 9-hydroxyphenalenone compound was prepared according to the reported procedure.¹³ The NMR spectra were recorded using a Bruker Avance 300 NMR spectrometer with a Bruker MAS 4 mm probehead. The NMR experiments were performed at 75.43 MHz for ^{13}C with a sample spinning speed of 9 kHz and a CP time of 1 ms. The selective excitation of resonance A or B was realized using a soft 90° pulse of 1025 μs . Temperatures of the sample were detected by a thermocouple on the inside near the air inlet of the probe housing, which were corrected with the chemical shift of the carboxyl carbon of samarium acetate.¹⁴ For CP under a high sample spinning condition, we used the RAMP CP method.¹⁵ The TPPM decoupling sequence¹⁶ was employed for more effective ^1H decoupling to yield the decoupling field of more than 75 kHz.

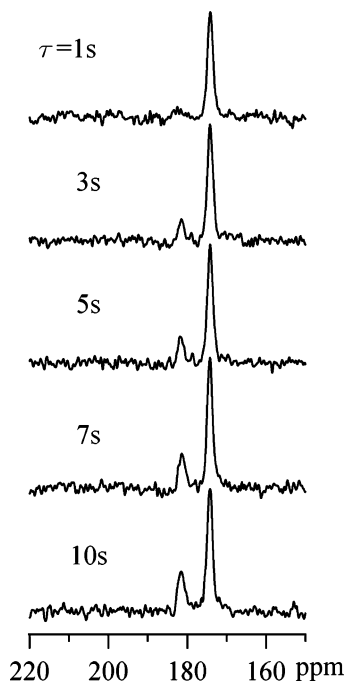


Figure 5. Variation in resonances A and B with the indicated exchange periods. These NMR spectra were measured at -70.6 °C using the 1D NMR pulse sequence in Figure 2. The ^{13}C magnetization for resonance B was locked in the $+z$ direction after CP.

4. Results and Discussion

Figure 4 shows the CP/MAS NMR spectra for 9-hydroxyphenalenone. They were measured in the range -97.7 to -1.1 °C. The splitting width of resonances A and B decreases with temperature, but it is still visible at room temperature (the spectrum at room temperature is not shown in this figure.).

9-Hydroxyphenalenone has a structural phase transition at $T_c = -18.2$ °C.^{1,2,17} In the low-temperature phase, it has four crystallographically independent molecules in the crystals.¹⁷ However, at -70.6 and -97.7 °C, resonances A and B do not show site splitting; each resonance can be considered as a single line. We can see from these results that these four molecules have almost the same potential curves in the low-temperature phase.

When the equilibrium constant, K , is equal to 1, the splitting width, $\delta\nu$, does not decrease with increasing exchange rate (i.e., with increasing temperature); the resonance lines gradually broaden with increasing temperature and finally coalesce into a single line.⁷ For the NMR spectra measured in this study, the splitting width, $\delta\nu$, decreases with temperature. The two resonance lines (i.e., resonances A and B) are not broadened except for those at -50.1 °C. The most likely explanation for the variation in $\delta\nu$ (with temperature) is as follows:

(a) The ratio, K , is less than 1 in the temperature range in which the CP/MAS measurements were performed.

(b) The exchange rates, k_1 and k_{-1} , increase with temperature, and the difference gradually approaches zero.

(c) As a result, the ratio, K , approaches 1 with temperature.

(d) Hence, the splitting width, $\delta\nu$, decreases with temperature according to $\delta\nu/\Delta\nu = (1 - K)/(1 + K)$.

As for the broadening at -50.1 °C, we must admit a still incomplete understanding of the observation—it may arise from the coexistence of different phases.

If the equilibrium constant, K , is equal to 1, it is easy to determine the stationary splitting width. The width, $\Delta\nu$, is given

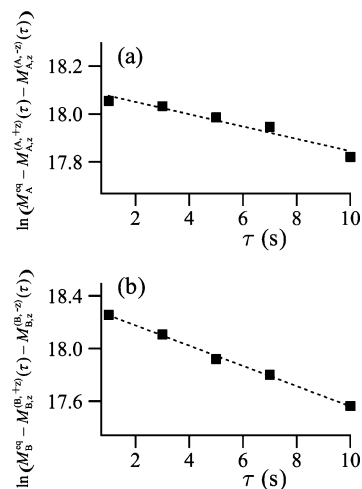


Figure 6. Plot of the experimental values of $\ln(M_A^{\text{eq}} - M_A^{(A,+z)}(\tau) - M_A^{(A,-z)}(\tau))$ and $\ln(M_B^{\text{eq}} - M_B^{(B,+z)}(\tau) - M_B^{(B,-z)}(\tau))$ vs the exchange period τ . For the definitions of these symbols, see the text. The lines drawn in the figure were determined by least-squares fits of the data. Their corresponding slopes yielded the relaxation rates for magnetizations A and B: $k_A = 0.026 \pm 0.003$ s $^{-1}$ and $k_B = 0.077 \pm 0.002$ s $^{-1}$.

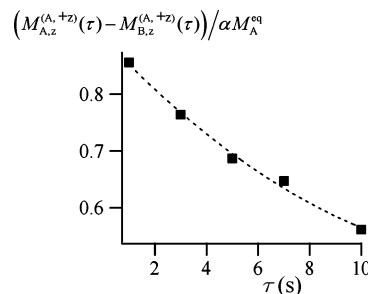


Figure 7. Plot of the experimental values of $(M_A^{(A,+z)}(\tau) - M_B^{(A,+z)}(\tau)) / \alpha M_A^{\text{eq}}$ vs the exchange period τ . See the text for the definitions of these symbols. A least-squares fit of the data to eq 10 produced the two quantities, P and Q , in eq 10. On the basis of these values, the rate constant, k_{-1} , the population, x_2 , and the equilibrium constant, K , were calculated.

by the expression of $k_{\text{coal}} = \pi \cdot \Delta\nu / \sqrt{2}$, where k_{coal} is the rate constant at a temperature when the chemical-shift difference becomes zero.¹⁸ On the contrary, the formalism is not available when $K < 1$. Therefore, it is necessary to adopt a new strategy to obtain the stationary splitting width for 9-hydroxyphenalenone.

Figure 5 shows the experimental ^{13}C NMR spectra recorded at -70.6 °C with the 1D NMR pulse sequence in Figure 2. The resonance lines for C1, called resonance A, gradually grow because of the spin relaxation and proton exchange. Thus the variation in these line intensities are generally described in terms of rate constants, T_{1A} , T_{1B} , $1/k_1$, and $1/k_{-1}$. To determine these rate constants, some methods have already been proposed in the field of liquid-state NMR;¹⁹ however, for the solid-state NMR, there have been few efforts to separately measure these rate constants.^{10,12}

Our new method is similar to that by Connor et al.¹² The latter method utilizes the chemical-shift difference to realize the situation where only one magnetization survives after a few dozen milli-seconds from the starting point of the exchange period. It should be noted that the method by Connor et al. can be applied only to the case in which the two exchange rates, k_1 and k_{-1} , are the same (i.e., the potential curve is symmetric) and in which the two relaxation rates, k_A and k_B , for two different

resonances are the same. The parameters dealt with in the method are $k_{\text{ex}} (=k_1 = k_{-1})$ and $k_{\text{relax}} (=k_A = k_B)$. In addition, the magnetization enhancements due to CP (hence, the difference in the CP efficiencies for the protonated and nonprotonated carbons) are not considered in the method.

For many 9-hydroxyphenalenone derivatives, the potential curves are asymmetric. In such occasions, the exchange rates, k_1 and k_{-1} , are different from each other. In addition, the two resonances generally have different relaxation rates, k_A and k_B . Therefore, a new method to separately determine these four rate constants is essential. The NMR method presented in this study can meet this demand; therefore, it is a new technology for the study of proton tautomerism in the solid state.

Plots of $\ln(M_A^{\text{eq}} - M_{A,z}^{(A,+z)}(\tau) - M_{A,z}^{(A,-z)}(\tau))$ and $\ln(M_B^{\text{eq}} - M_{B,z}^{(B,+z)}(\tau) - M_{B,z}^{(B,-z)}(\tau))$ versus the exchange period τ are shown in Figure 6 (see eq 7). The experimental data were acquired from the 1D spin exchange NMR experiments: the measurements of the line intensities for resonance A(B) after magnetization A(B) is locked in the $+z$ or $-z$ direction. Least-squares fits of the data points, which are represented by the dotted curves, yielded the two relaxation rates for magnetizations A and B; i.e., $k_A = 0.026 \pm 0.003 \text{ s}^{-1}$ and $k_B = 0.077 \pm 0.002 \text{ s}^{-1}$.

In our previous study,²⁰ the splitting width, $\delta\nu$, was found to asymptotically approach 11.5 ppm with decreasing temperature. Because $\delta\nu$ at $-70.6 \text{ }^\circ\text{C}$ is 7.26 ppm, if the stationary splitting width of 9-hydroxyphenalenone is assumed to be around 12 ppm, then the equilibrium constant K at $-70.6 \text{ }^\circ\text{C}$ is ca. 0.23 from eq 1. It is likely that the exchange rate, k_{-1} , is on the order of 0.1 s,¹⁰ so that the exchange rate, k_1 , will be on the order of 0.01 s. On the basis of these results, eq 9 can be expanded as

$$(M_{A,z}^{(A,+z)}(\tau) - M_{B,z}^{(A,+z)}(\tau))/\alpha M_A^{\text{eq}} = 1 - P\tau + Q\tau^2 \quad (10)$$

where $P = 2x_2k_{-1}$ and $Q = (1/4)Pk_{-1}$.

Figure 7 shows the variation in $(M_{A,z}^{(A,+z)}(\tau) - M_{B,z}^{(A,+z)}(\tau))/\alpha M_A^{\text{eq}}$ versus the exchange period τ . The data were also obtained from the 1D spin exchange NMR measurements. On the basis of the discussions in the preceding paragraph, the data points were least-squares fitted to eq 10. The values thus obtained for P and Q are $0.048 \pm 0.007 \text{ s}^{-1}$ and $0.0015 \pm 0.0006 \text{ s}^{-2}$, respectively. On the basis of these results, the following parameters are derived: $k_{-1} = 0.12 \pm 0.0 \text{ 5s}^{-1}$, $x_2 = 0.20 \pm 0.08$, and $x_1 = 0.80 \pm 0.08$ (x_1 is determined from the relation of $x_1 + x_2 = 1$). It follows from the populations that the equilibrium constant, K , is 0.25 ± 0.10 at $-70.6 \text{ }^\circ\text{C}$; this result ($K < 1$) indicates that the potential curve is unsymmetrical with respect to its saddle point.⁷ Using the values for K and $\delta\nu$ at $-70.6 \text{ }^\circ\text{C}$ ($\delta\nu = 7.26 \text{ ppm}$ at $-70.6 \text{ }^\circ\text{C}$), we have found $\Delta\nu = 12.1 \pm 2.6 \text{ ppm}$ for the stationary splitting width. This value is very close to the above estimation (11.5 ppm) for 9-hydroxyphenalenone. This result would provide confirmation that the present NMR method can adequately determine the stationary splitting width, $\Delta\nu$.

5. Conclusion

In this study, we tried to obtain detailed information on the potential curve for the proton tautomerism in solid 9-hydroxyphenalenone. The proton tautomerism had a significant effect on the ^{13}C chemical-shift difference between resonances A and B (C1 and C9). The most important factor for attaining the objective of this study was to acquire the stationary splitting width (i.e., the ^{13}C chemical-shift difference when the proton tautomerism is completely frozen.)

First, we presented a new NMR method to separately determine the rate constants for the spin relaxation and proton exchange. Using this method at $-70.6 \text{ }^\circ\text{C}$, we obtained the exchange rate, k_{-1} , and populations, x_2 and x_1 , related to the proton tautomerism. The stationary splitting width was then calculated by using the equilibrium constant, K , and the shift difference, $\delta\nu$, at $-70.6 \text{ }^\circ\text{C}$.

It is particularly worth noting that the stationary splitting width was found at a relatively high temperature where the tautomerism is still active and where a stable and fast sample spinning is feasible. The stationary splitting width determined by this method seemed to be very close to the estimate for 9-hydroxyphenalenone. Therefore, our new method will be of great utility for research aimed at important tautomers such as the 9-hydroxyphenalenone derivatives.

Acknowledgment. A part of the experimental work was carried out at the Hosei University Research Center for Micro-Nano Technology. We thank Prof. H. Ogata for use of the Bruker Avance 300 NMR spectrometer.

References and Notes

- Mochida, T.; Izuoka, A.; Sugawara, T.; Morimoto, Y.; Tokura, Y. *J. Chem. Phys.* **1994**, *100*, 6646.
- Mochida, T.; Izuoka, A.; Sugawara, T.; Morimoto, Y.; Tokura, Y. *J. Chem. Phys.* **1994**, *101*, 7971.
- Mochida, T.; Kuwahara, D.; Miyajima, S.; Sugawara, T. *J. Phys. Chem. B* **2003**, *107*, 12315.
- Sugawara, T.; Takasu, I. *Adv. Phys. Org. Chem.* **1999**, *32*, 219.
- Limbach, H. H.; Hennig, J.; Kendrick, R.; Yannoni, C. S. *J. Am. Chem. Soc.* **1984**, *106*, 4059.
- Limbach, H. H.; Wehrle, B.; Schlabach, M.; Kendrick, R.; Yannoni, C. S. *J. Magn. Reson.* **1988**, *77*, 84.
- Braun, J.; Schlabach, M.; Wehrle, B.; Köcher, M.; Vogel, E.; Limbach, H. H. *J. Am. Chem. Soc.* **1994**, *116*, 6593.
- <http://www.dotynmr.com>.
- Jeener, J.; Meier, B. H.; Bachmann, P.; Ernst, R. R. *J. Chem. Phys.* **1979**, *71*, 4546.
- Szeverenyi, N. M.; Bax, A.; Maciel, G. E. *J. Am. Chem. Soc.* **1983**, *105*, 2579.
- Freeman, R. *A Handbook of Nuclear Magnetic Resonance*, 2nd ed.; Harlow: London, 1997.
- Connor, C.; Naito, A.; Takegoshi, K.; McDowell, C. A. *Chem. Phys. Lett.* **1985**, *113*, 123.
- Haddon, R. C. *J. Org. Chem.* **1986**, *46*, 4588.
- Campbell, G. C.; Crosby, R. C.; Haw, J. F. *J. Magn. Reson.* **1986**, *69*, 191.
- Metz, G.; Wu, X.; Smith, S. O. *J. Magn. Reson. A* **1994**, *110*, 219.
- Bennett, A. E.; Rienstra, C. M.; Auger, M.; Lakshmi, K. V.; Griffin, R. G. *J. Chem. Phys.* **1995**, *103*, 6951.
- Svensson, C.; Abrahams, S. C. *Acta Crystallogr. B* **1986**, *42*, 280.
- Akitt, J. W. *NMR and Chemistry. An Introduction to Modern NMR Spectroscopy*, 3rd ed.; Chapman & Hall: London, 1992.
- Hennig, J.; Limbach, H. H. *J. Magn. Reson.* **1982**, *49*, 322 and references therein.
- Mochida, T. Ph.D. Thesis, The University of Tokyo, Tokyo, 1994.